Effect of in-Mold Electromagnetic Stirring on Solidification and Inclusion Behavior

Rajneesh Kumar and Pradeep Kumar Jha

October 24, 2022

4th International Conference on Science and Technology of Ironmaking and Steelmaking
13-16 Dec. 2022
IIT Bombay, Mumbai, India

Effect of in-mold electromagnetic stirring on solidification and inclusion behavior

Rajneesh Kumar, Pradeep Kumar Jha
Department of Mechanical and Industrial Engineering, IIT Roorkee, Roorkee-247667, India
rajneeshkumar0678@gmail.com, pradeep.jha@me.iitr.ac.in

Abstract

A three-dimensional transient model of in-mold electromagnetic stirring in bloom continuous casting mold has been developed. Time-varying electromagnetic field has been coupled with fluid flow, solidification and inclusion tracking model to investigate the effect of electromagnetic stirring on solidification and non-metallic inclusion behavior. The realizable k-ε turbulence model and the enthalpy-porosity approach have been used to investigate the fluid flow and the solidification of liquid steel in the mold. The behavior of non-metallic inclusions is analyzed using the stochastic tracking model. Electromagnetic stirring inhibits initial solid shell formation at the mold wall and turns the liquid core at the strand's center into a liquid-solid interface mush. Analysis has also been done on the impact of inclusion size and density on the removal rate of non-metallic inclusions. The findings indicate that inclusion and solidification behavior is significantly influenced by in-mold EMS.

Keywords: solidification, inclusion, mold, electromagnetic stirring

1. INTRODUCTION

Continuous casting is a widely used process for steel-making. Molten metal is fed into a water-cooled copper mold through the tundish. The heat is extracted from the molten metal by the mold in the primary cooling zone, forming the solid shell at the perimeter of the mold. After sufficient thickness is attained to sustain the ferrostatic pressure exerted by the molten metal [1], the semi-solidified strand is withdrawn from the mold by the rollers. Further cooling takes place by the water spray in the secondary cooling zone. After the strand is fully solidified, it is cut by the torch into the desired length. The continuous casting process of steel is shown in **Fig 1(a)**.

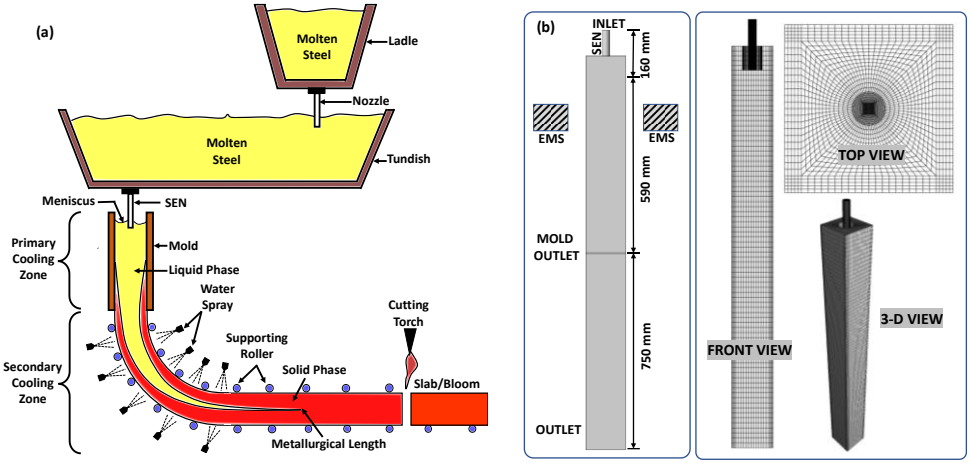

Fig. 1: Schematic of (a) the continuous casting process and (b) geometry used for EM field generation and mold grid details

During the process, many chemical reactions take place, forming oxides, sulfides, nitrides, carbides, and their compounds into the molten metal [2]. This acts as the impurities in the form of inclusions in the molten metal, which deteriorate the surface and sub-surface quality of the products. The flow patterns can remove the inclusion from the molten metal [3, 4] and improve the microstructure of final products [5]. There are various methods by which the flow patterns are improved or altered, such as mold design, SEN design, and casting conditions (casting speed, superheat, SEN depth etc.) [5]. Role of EMS is also reported by the researchers in changing the flow in real-time and improve the

microstructure (transition of columnar to equiaxed) of the casting [6], [7].

A number of researchers numerically investigated the inclusion motions inside the molten metal, removal of these inclusions by the slag layer and their entrapment into the solidified shell [8–13]. Few investigations were also carried out in the bloom and billets [11,13,14]. Very few work reported regarding development of model by coupling the EMS, transient flow, solidification and inclusion tracking phenomena. The effect of time-varying EMS has not been reported on the inclusion behavior inside the billet mold. Hence, investigation in this domain is highly desired.

The present investigation aims to develop a 3-D numerical model by coupling the time-varying electromagnetic field with the transient flow, solidification and inclusion tracking in the billet mold. The effect of EMS on the flow, solidification and inclusion motion, removal and entrapment is investigated. The effect of inclusion size and density is also studied on the inclusion behavior with and without EMS. The validation of model is reported in earlier work by authors [11].

2. PROBLEM DESCRIPTION AND METHODOLOGY

This article considers a bloom mold with a bifurcated submerged entry nozzle (SEN). The cross-section area of the mold is 150 mm x 150 mm and the effective length of the mold is 750 mm. The total length of the computation domain is 1500 mm. The stirrer is placed 300 mm below the meniscus to develop the magnetic field in the mold. **Fig. 1(b)** shows the schematic of the mold geometry used to find out the magnetohydrodynamics (MHD). The stirrer consists of six poles placed at 60 degrees from each other. The three-phase alternating current is supplied to the stirrer to produce the electromagnetic (EM) field. The internal and external diameter of the SEN is 30 mm and 70 mm, respectively. The core length and diameter of the stirrer is 200 mm and 425 mm, respectively. Mesh used in the investigation is shown in **Fig. 1(b)**. After grid sensitivity analysis, the base grid having 197200 elements was selected for the present investigation.

The simulation analysis has been carried out in three stages. In the first stage, a time-varying magnetic field is calculated in the mold using the Ansys EM Suite. This magnetic field data is converted into the required format compatible with the Ansys Fluent. In the second stage, this data is coupled with the turbulent flow to analyze the MHD in the mold. In this stage, the solidification model is also coupled with MHD. When the simulation reaches a quasi-steady state, the discrete phase model (DPM) with user-defined functions is used to determine the inclusions motion in the final stage [11,13].

Based on the casting speed (2.1 m/s), the inlet velocity is calculated using mass conservation between the inlet and output, and the inlet temperature is established as the sum of the liquidus temperature and the superheat. The semi-empirical equations compute the turbulent kinetic energy and dissipation rate at the inlet [11,13]. Velocity outlet boundary condition is set at the mold outlet [11,15]. Free slip and no-slip conditions are set at the meniscus and walls of the mold and SEN, respectively [11]. The heat flux (W/m^2) on the mold wall is applied according to the Savage and Pritchard equation [16]. The strand wall has an average heat transfer coefficient of 850 W/m^2K. The physical properties used in the present analysis are provided in reported literature [11].

Shape of inclusion particles is assumed to be spherical. Through the SEN inlet, 6600 inclusion particles are injected into the mold as a surface injection at the same velocity as the molten steel. The inclusions are set to be trapped at the meniscus if they touch it. Escape condition is applied at the mold outlet. If the inclusion size is smaller than the primary dendrite arm spacing (PDAS), they are entrapped/engulfed into the solidified shell.

3. RESULTS AND DISCUSSION

3.1 Magnetic field density distribution

Fig. 2(a) shows the magnetic field density (MFD) distribution along the centerline of the strand. The stirrer current and frequency is 450 A and 2 Hz, respectively. The MFD is maximum at the center of the stirrer and decreases on both sides symmetrically. It is almost vanishing below the mold. The maximum magnitude of MHD is 249.96 mT observed at the center of the stirrer. Due to this maximum tangential velocity of the molten fluid is reached at the center plane of the stirrer.

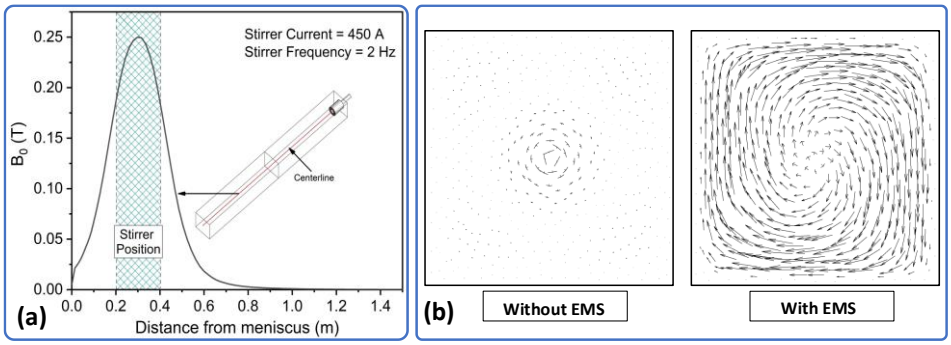

Fig. 2: (a) MFD distribution at the center of the domain and (b) velocity vector at stirrer center plane under the effect of without and with EMS

3.2 Effect on fluid flow

Fig. 2(b) compares the velocity vectors at the cross-section plane 300 mm below the meniscus (top surface of the mold) with and without EMS. When EMS is not presented, the vector is almost shown in the form of a dot. This is because the velocity in the x and y direction is nearly zero and the molten metal flows in the z direction only. However, under the influence of EMS, the swirl flow is developed in a clockwise direction. Due to swirl flow, the x-y direction velocity components are most prominent compared to without EMS, which also decreases the velocity in the z direction. At the perimeter of the mold, the velocity component is shown in the form of a dot, which is due to the solidified shell moving in z direction with casting speed.

Fig. 3(a) shows the velocity contour at the strand's center plane (y=0) and the 3-D streamline of fluid flow inside the computational domain under the influence of without and with EMS. In a case without EMS, the flow that comes out from the SEN directly flows into the core of the mold without having any hindrance. Further, it forms the recirculation zone in the upper half of the mold. The molten steel is flowing in an upward direction along the mold surface in the recirculation zone. The intensity of flow coming out through the SEN is prominently affected by the swirl flow developed due to the application of the EMS. The EMS significantly affects the flow inside the mold, as shown in **Fig. 3(a)**. The effect of EMS is limited inside the mold, as illustrated by the streamlined diagram.

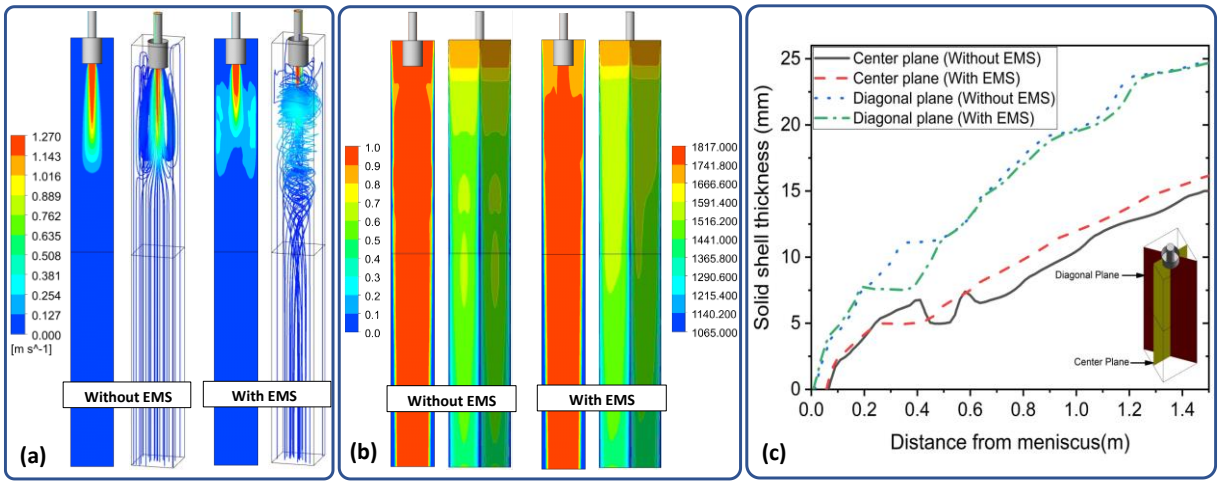

Fig. 3: (a) Velocity contour and streamline of flow in the domain, (b) liquid fraction and temperature contour, and (c) solid shell thickness under the effect of without and with EMS.

3.3 Effect on solidification

Fig. 3(b) shows the liquid fraction at the center plane (y=0) of the strand and temperature contour on the wall of the strand under the effect of without and with EMS. The liquid fraction is higher in the upper zone of the mold near the meniscus compared to the EMS. The stirrer effectively distributes the temperature in the entire domain due to the swirl flow. This also increases the residence time interval

of the molten metal inside the domain. Therefore, the heat extraction rate through the mold wall increases significantly, as shown in **Fig. 3(b)**. In the case of stirrer current value as zero, there is a hot spot on the wall of the mold. Further, it is absent in the cases having stirrer current due to uniform heat extraction from the mold wall.

The effect of EMS on the solidification is effectively analyzed by the solid shell thickness developed at the periphery of the mold. In the case without EMS, the solid shell thickness (center plane) is either almost equal to or greater than the thickness formed under the influence of EMS from z=0 m to z=0.41 m, as shown in **Fig. 3(c)**. This is due to the formation of a recirculation zone in that region. Further, this increases the heat extraction rate from the molten metal and promotes the formation of solid shell thickness. Moreover, the temperature of the core of the molten metal is higher due to molten metal directly flowing into that region through the SEN, as shown in **Fig. 3(a)**. Due to the high temperature of the molten metal, the solid shell remelts (z=0.42 m) and then progressively increases. In the case of a stirrer, the remelting and breakdown of the solidified shell occur from z=0.2 m to z=0.4 m due to the high intensity of swirling flow in that region. The mushy zone formed at the perimeter of the mold gets mixed with the molten metal due to swirl flow. This drops the temperature and liquid fraction of the molten metal, which promotes the formation of the solid shell thickness. At the strand outlet, the thickness of the solidified shell is more in the case of EMS at the center plane, as shown in **Fig. 3(c)**. However, the thickness of the solid shell is not significantly affected by the EMS at the corner of the mold except in the stirrer region.

3.4 Effect on inclusion behavior

The inclusion motion, removal and entrapment into the computational domain are investigated without and with the influence of EMS. The different inclusion sizes 10 µm, 50 µm and 100 µm is denoted as s_1, s_2 and s_3, respectively. The inclusion densities of 2600 kg/m^3, 3700 kg/m^3 and 4600 kg/m^3 are denoted by the ρ_1, ρ_2 and ρ_3, respectively. **Figs. 4(a)** and **4(b)** show the transient position of the inclusion injected through the SEN inlet as a surface injection into the molten metal without and with EMS. In this figure, the light grey portion shows the iso-plane of the solid shell thickness at the 0.3 liquid fraction. Additionally, 1 to 4 in **Figs. 4(a-b)** signifies the position of the inclusion at time interval of 1 second, 5 seconds, 15 seconds and 35 seconds, respectively. **Figs. 4(a)(5)** and **4(b)(5)** shows the inclusion entrapment into the solidified shell. The s_3 and ρ_2 type inclusion is considered in **Figs. 4(a)** and **4(b)**.

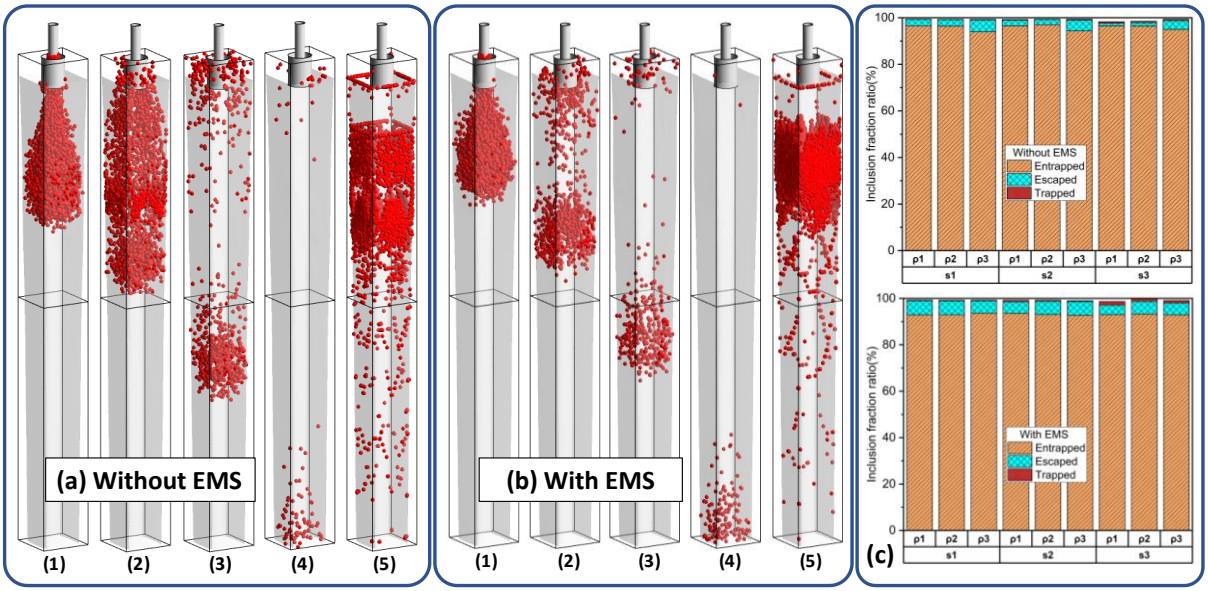

Fig. 4: Transient inclusion position inside the molten metal at different time intervals (a) without EMS, (b) with EMS, and (c) inclusion fraction ratio for a different size and density of inclusion.

The flow of inclusion deep into the mold is restricted in the case of EMS compared to without EMS due to the swirl flow. Most of the particle is uniformly distributed in the case of a stirrer. The entrapped inclusion into the solidified shell is moving with the shell in a downward direction with the

casting speed. In the case of EMS, the entrapped inclusion is again flowed into the molten steel due to the washing effect and increases the possibility of the inclusion removed by the slag layer.

Fig. 4(c) shows the inclusion fraction ratio for different sizes and densities of inclusion under the influence of without and with EMS. In the case of EMS, the fraction of inclusion entrapped into the solid shell is decreased as compared to without EMS. This is due to the washing effect of swirl flow. The swirl flow washes the inclusion entrapped into the solidified shell, and the inclusion again flows into the molten metal. This increases the probability of the inclusions being removed by the slag layer. The fraction of inclusion removed by the slag layer increases with the inclusion size. However, the fraction of inclusion escaped through the strand outlet decreases. This is due to increased buoyancy force because of increase in the inclusion size. The density of inclusion also has a great impact on inclusion motions. With an increase in inclusion density, the removal rate decreases and the inclusion escaped through the mold outlet increases. The proper distribution of inclusion takes place under the influence of EMS and inhibits the inclusion cluster formation.

4. CONCLUSIONS

The EMS suppressed the molten steel flow coming out from SEN and changed the flow pattern inside the mold into swirl flow. It promotes the formation of solid shell at the center plane, while not significantly affecting at the corner of the strand. The larger size and smaller density of inclusion has greater tendency to move upwards direction due to buoyancy force and removed by the slag layer. The EMS promotes the proper distributions of inclusion inside the molten steel and promotes the inclusions removal rate by development of swirl flow, that washes the entrapped inclusions from the solidified shell.

REFERENCES

[1] A. Akni, A. Bellaouar, M. Lachi, Numerical modeling of the flow in the mold of the continuous casting machine, Heat and Mass Transfer. 49 (2013) 1039–1050.
[2] Y. Sahai, Tundish Technology for Casting Clean Steel: A Review, Metallurgical and Materials Transactions B. 47 (2016) 2095–2106.
[3] Y.H. Ho, W.S. Hwang, Numerical simulation of inclusion removal in a billet continuous casting mold based on the partial-cell technique, ISIJ International. 43 (2003) 1715–1723.
[4] B. Li, H. Lu, Y. Zhong, Z. Ren, Z. Lei, Numerical simulation for the influence of EMS position on fluid flow and inclusion removal in a slab continuous casting mold, ISIJ International. 60 (2020) 1204–1212.
[5] S. Cho, B.G. Thomas, Electromagnetic forces in continuous casting of steel slabs, Metals. 9 (2019) 1–38.
[6] A. Maurya, P.K. Jha, Analysis of solidification kinetics in mold during continuous casting process, in: Manufacturing Techniques for Materials (2018) 539–557.
[7] A. Maurya, P.K. Jha, Study of fluid flow and solidification in billet caster continuous casting mold with electromagnetic stirring, Archives of Metallurgy and Materials. 63 (2018) 413–424.
[8] Y. bin Yin, J. ming Zhang, Large eddy simulation of transient transport and entrapment of particle during slab continuous casting, Journal of Iron and Steel Research International. 29 (2022) 247–262.
[9] L. Zhang, Y. Wang, X. Zuo, Flow transport and inclusion motion in steel continuous-casting mold under submerged entry nozzle clogging condition, Metallurgical and Materials Transactions B. 39B (2008)
[10] C. Pfeiler, B.G. Thomas, M. Wu, A. Ludwig, A. Kharicha, Solidification and particle entrapment during continuous casting of steel, Steel Res Int. 79 (2008) 599–607.
[11] R. Kumar, P.K. Jha, Numerical simulation for EMS induced solidification and inclusion behavior in bloom caster CC mold with bifurcated SEN, J Manuf Process. 81 (2022) 396–405.
[12] Y. Yin, J. Zhang, H. Ma, Q. Zhou, Large eddy simulation of transient flow, particle transport, and entrapment in slab mold with double-ruler electromagnetic braking, Steel Res Int. 92 (2021) 1–11.
[13] R. Kumar, P.K. Jha, Effect of casting speed on solidification and inclusion motions in bloom mold caster under the influence of in-mold electromagnetic stirring, Int J Numer Methods Heat Fluid Flow. (2022).
[14] Y. Yin, J. Zhang, Q. Dong, Q.H. Zhou, Mathematical modelling of inclusion motion and entrapment in billet mould with effect of electromagnetic stirring, Ironmaking and Steelmaking. 46 (2019) 855–864.
[15] A. Maurya, R. Kumar, P.K. Jha, Simulation of electromagnetic field and its effect during electromagnetic stirring in continuous casting mold, J Manuf Process. 60 (2020) 596–607.
[16] J. Savage, W.H. Pritchard, The problem of rupture of the billet in the continuous casting of steel, Journal of Iron Steel Inst. 178 (1954) 269–277.